TRANSITIONAL OBJECT'S SHAPE SIMULATION BY LAGRANGE'S EQUATION AND FINITE ELEMENT METHOD

Raquel R. Pinho João M. R. S. Tavares
LOME – Laboratório de Óptica e Mecânica Experimental
FEUP – Faculdade de Engenharia da Universidade do Porto
Rua Dr. Roberto Frias, s/n, 4200-465 Porto
Portugal
{rpinho, tavares}@fe.up.pt

Abstract
This paper presents a methodology to obtain transitional objects' shapes by a physics-based simulation. Given two 2D/3D images of different objects or of the same object at different instants, using the Finite Element Method two models are built, and the Lagrange's equation is solved to simulate the involved deformation. We used and compared two different finite elements to build each objects' model: the Sclaroff's isoparametric element and the linear axial element.

Keywords
Deformable Objects, Movement/Deformation Simulation, Matching, Finite Element Method, Lagrange's Equation, Modal Analysis.

1. INTRODUCTION

To obtain transitional objects' shapes, several techniques may be used. However, not all the obtained results are coherent with the objects' physical properties. To physically simulate objects' movement/deformation we use an approach that builds physical models for each given object, through the Finite Element Method (FEM), and then solve Lagrange's Equation (LE) (figure 1).
We have attended to what has already been done by solving LE among deformable objects' images, such as the analytical determination of vibration modes by Nastar in [1], [2], [3], the isoparametric finite element developed by Sclaroff to model objects by the FEM in [4], [5], and the study done by Tavares with real objects' images, who also used Sclaroff's isoparametric element and groups of linear axial elements to build the objects models in [6], [7].
To build the object's physical models with the FEM we use grouped linear axial elements [6], [8] or Sclaroff's isoparametric element [4], [5], [6]. In this paper we compare the transitional objects' shapes obtained by each used model.
To match the shapes' nodes we use modal analysis [4],

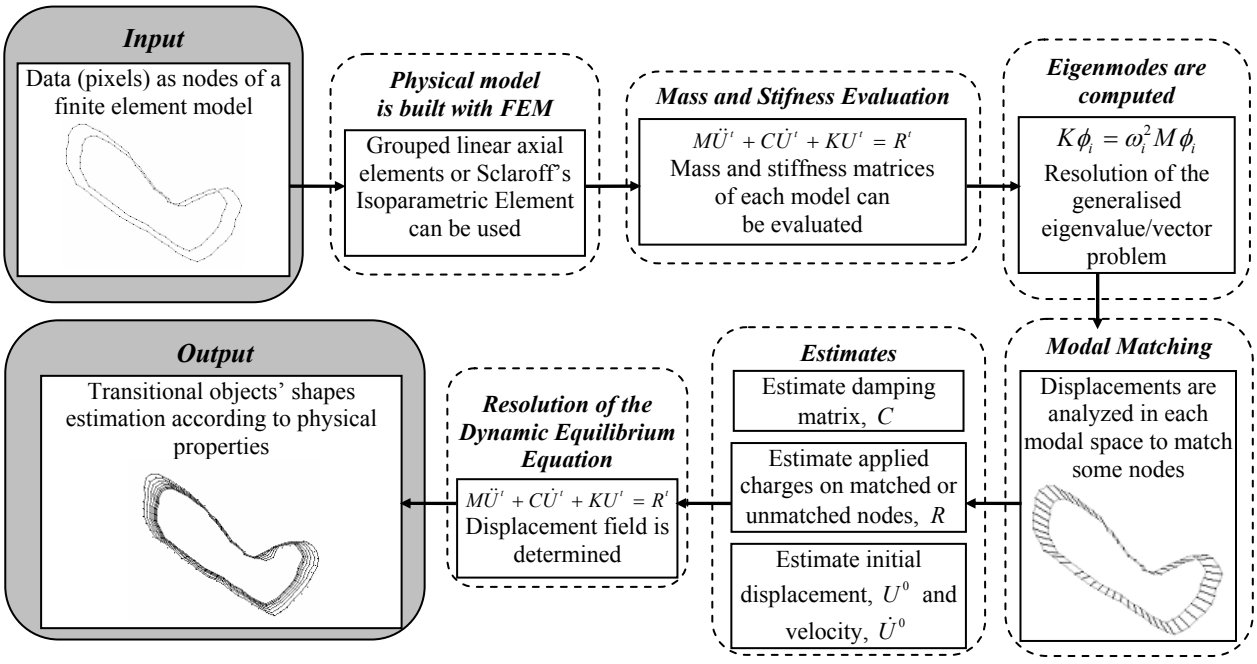

Figure 1: Diagram of the approach used to estimate transitional objects' shapes.

[5], [6], [7], [9], [10], which generally obtains satisfactory matching results although not all nodes may be successfully matched. However, to solve LE all nodes should be matched, so we propose a solution based on the neighbourhood criterion that overcomes this matching problem.

To solve LE we did not consider any additional information about the represented objects or of the movement/deformation involved, and so we had to estimate the initial displacement and velocity, as well as the implicit applied charges. In this paper we also mention how these required parameters were estimated.

This approach can be used to do physics-based morphing, to reconstruct 3D objects from 2D slices, to simulate objects collision, to interpolate objects data, etc.

2. FINITE ELEMENTS USED

In the presented work we considered two different object's type: 2D contour and 3D surface.

To model each given object we applied the FEM by using Sclaroff's isoparametric element or a group of linear axial elements [6].

Using Sclaroff´s isoparametric finite element, the built models for the given 2D contours delimit a virtual object with elastic properties, and the obtained model is like an elastic membrane [4], [6]. When a 3D surface object is modelled by the same element, it is as if each feature point is covered by a blob of rubbery material [4], [6]. Instead, if a group of linear axial elements is used to build the 2D/3D models, then the contours/surfaces are shallow models whose edges are 1D finite elements. So, all the cells interiors are ignored [4], [6].

When a shape is modelled with Sclaroff's isoparametric element, it is not necessary to determine the pixels order; however, when linear axial elements are used, it is necessary to determine the pixels correct order, so that the grouping is correctly made [6]. In this case, to obtain the correct order, a 2D Delaunay algorithm can be used [6], [11].

To build the Sclaroff's element interpolation matrix H (which relates the distances between objects' nodes) Gaussian functions are used:

$$g_i(X) = e^{-\|X - X_i\|^2 / (2\sigma^2)},$$

where X_i is the function's n-dimensional center, and σ its standard deviation (which controls data interaction). The interpolation functions, h_i, are then given by:

$$h_i(X) = \sum_{k=1}^{m} a_{ik}\, g_k(X),$$

where a_{ik} are the interpolation coefficients, with value 1 (one) at node i, and 0 (zero) at all other nodes, and m is the number of nodes.

The interpolation coefficients a_{ik} can be determined by inverting matrix G defined as:

$$G = \begin{bmatrix} g_1(x_1) & \cdots & g_1(x_m) \\ \vdots & \ddots & \vdots \\ g_m(x_1) & \cdots & g_m(x_m) \end{bmatrix}.$$

This way, the interpolation matrix of Sclaroff's isoparametric element, for a 2D shape will be:

$$H(X) = \begin{bmatrix} h_1 & \cdots & h_m & 0 & \cdots & 0 \\ 0 & \cdots & 0 & h_1 & \cdots & h_m \end{bmatrix}.$$

The mass and stiffness matrices, M and K respectively, are then built as usually [4], [5], [6], [9]. Thus, for 2D shapes we obtain:

$$M = \begin{bmatrix} M_{aa} & 0 \\ 0 & M_{aa} \end{bmatrix} \text{ and } K = \begin{bmatrix} K_{aa} & K_{ab} \\ K_{ba} & K_{bb} \end{bmatrix},$$

where

$$M_{aa_{ij}} = \rho\pi\sigma^2 \sum_{k,l} a_{ik} a_{jl} \sqrt{g_{kl}},$$

$$K_{ab_{ij}} = K_{ba_{ij}} = -\frac{\pi\beta(\alpha+\xi)}{4\sigma^2} \sum_{k,l} a_{ik} a_{jl} \hat{x}_{kl} \hat{y}_{kl} \sqrt{g_{kl}},$$

$$\hat{x}_{kl} = (x_k - x_l),\ \hat{y}_{kl} = (y_k - y_l),$$

and ρ is the material's density, α, β and ξ are obtained from material modulus of elasticity, E, and Poisson's ratio, υ:

$$\alpha = \frac{\upsilon}{1-\upsilon},\ \beta = \frac{E(1-\upsilon)}{(1+\upsilon)(1-2\upsilon)},\ \text{and } \xi = \frac{1-2\upsilon}{2(1-\upsilon)}.$$

For a 3D shape, H will be [4], [5], [6]:

$$H(x) = \begin{bmatrix} h_1 & \cdots & h_m & 0 & \cdots & 0 & 0 & \cdots & 0 \\ 0 & \cdots & 0 & h_1 & \cdots & h_m & 0 & \cdots & 0 \\ 0 & \cdots & 0 & 0 & \cdots & 0 & h_1 & \cdots & h_m \end{bmatrix},$$

and the 3D Sclaroff's isoparametric element mass matrix will be defined as:

$$M = \begin{bmatrix} \mathrm{M} & 0 & 0 \\ 0 & \mathrm{M} & 0 \\ 0 & 0 & \mathrm{M} \end{bmatrix},$$

where

$$\mathrm{M} = \rho\pi^{\frac{3}{2}}\sigma^3 A^T \sqrt{G} A = \rho\pi^{\frac{3}{2}}\sigma^3 G^{-1}\sqrt{G}G^{-1},$$

the elements of $\sqrt{G}$ are the square roots of G's elements, and the stiffness matrix is given by:

$$K = \begin{bmatrix} K_{11}^T & K_{12}^T & K_{13}^T \\ K_{21}^T & K_{22}^T & K_{23}^T \\ K_{31}^T & K_{32}^T & K_{33}^T \end{bmatrix},$$

where K_{ij}^T are symmetric submatrices given by:

$$K_{11_{ij}} = \pi^{\frac{3}{2}}\sigma\beta \sum_{k,l} a_{ik} a_{jl} \left[\frac{1+\xi}{2} - \frac{\hat{x}_{kl}^2 + \xi(\hat{y}_{kl}^2 + \hat{z}_{kl}^2)}{4\sigma^2} \right] \sqrt{g_{kl}},$$

$$K_{22_{ij}} = \pi^{\frac{3}{2}}\sigma\beta \sum_{k,l} a_{ik} a_{jl} \left[\frac{1+\xi}{2} - \frac{\hat{y}_{kl}^2 + \xi(\hat{x}_{kl}^2 + \hat{z}_{kl}^2)}{4\sigma^2} \right] \sqrt{g_{kl}},$$

$$K_{33_{ij}} = \pi^{\frac{3}{2}}\sigma\beta\sum_{k,l} a_{ik}a_{jl}\left[\frac{1+\xi}{2} - \frac{\hat{z}_{kl}^2 + \xi(\hat{x}_{kl}^2 + \hat{y}_{kl}^2)}{4\sigma^2}\right]\sqrt{g_{kl}}\ ,$$

$$K_{12_{ij}} = -\frac{\pi^{\frac{3}{2}}\beta(\alpha+\xi)}{4\sigma}\sum_{k,l} a_{ik}a_{jl}\hat{x}_{kl}^2\hat{y}_{kl}^2\sqrt{g_{kl}}\ ,$$

$$K_{13_{ij}} = -\frac{\pi^{\frac{3}{2}}\beta(\alpha+\xi)}{4\sigma}\sum_{k,l} a_{ik}a_{jl}\hat{x}_{kl}^2\hat{z}_{kl}^2\sqrt{g_{kl}}\ ,$$

and

$$K_{23_{ij}} = -\frac{\pi^{\frac{3}{2}}\beta(\alpha+\xi)}{4\sigma}\sum_{k,l} a_{ik}a_{jl}\hat{y}_{kl}^2\hat{z}_{kl}^2\sqrt{g_{kl}}\ .$$

The determination of the mass and stiffness matrices for the group of axial linear elements is a FEM standard and usual process (see for example [6], [8], [12]).

The used damping matrix, C, is a linear combination of the mass and stiffness matrices:

$C = \hat{\alpha}M + \hat{\beta}K$,

where $\hat{\alpha}$ and $\hat{\beta}$ are respectively the mass and stiffness constraints determined by the desired critical damping [13].

3. MODAL MATCHING

To match the initial and target shapes nodes, each generalized eigenvalue/vector problem is solved:

$K\Phi = M\Phi\Omega$,

where for a 2D model with m nodes:

$$\Phi = \left[\phi_1 \mid \cdots \mid \phi_{2m}\right] = \begin{bmatrix} u_1^T \\ \vdots \\ u_m^T \\ v_1^T \\ \vdots \\ v_m^T \end{bmatrix}, \text{ and } \Omega = \begin{bmatrix} \omega_1^2 & & 0 \\ & \ddots & \\ 0 & & \omega_{2m}^2 \end{bmatrix}.$$

The mode i shape vector, ϕ_i, describes the displacement (u, v) of each node due to the vibration mode *i*, and in the diagonal matrix Ω the frequency of vibrations' squares are increasingly ordered.

After building each modal matrix, by comparing the displacement of each node in the respective modal eigenspace, some nodes can be matched. To do so, an affinity matrix, Z, is built with entries:

$Z_{ij} = \left\|u_{1,i} - u_{2,j}\right\|^2 + \left\|v_{1,i} - v_{2,j}\right\|^2$,

and best matches are indicated by the minimum values of associated lines and columns. The affinity between nodes i and j will be 0 (zero) if the match is perfect, and will increase as the match worsens.

The process of matching 3D shapes is entirely analogous [4], [6].

4. RESOLUTION OF THE DYNAMIC EQUILIBRIUM EQUATION

In this work, to obtain the transitional objects' shapes attending to physical properties we solve the Lagrange's Equation:

$M\ddot{U}^t + C\dot{U}^t + KU^t = R^t$, (1)

with the nodal displacements, U, described as:

$U_i = X_{2,i} - X_{1,i}$,

where $X_{1,i}$ is the position of the i^{th} node in the initial shape and $X_{2,i}$ in the target one, and U_i is the associated displacement.

To solve the dynamic equilibrium equation several integration methods can be used. In this paper, we present results obtained by the Mode Superposition Method [9], [10], [12], [13].

4.1. Mode Superposition Method

This method allows the resolution of LE (1) using only part of the model's modes in the computation process. This measure reduces the computational cost because it despises the movement's local components, essentially associated to noise. This way, the computation involved is accelerated without great loss of information as generally the high order frequency modes have very little effect on the movement [4], [6].

The Mode Superposition Method proposes the transformation between the generalized coordinates, Φ used to transform the modal displacements, X, into nodal displacements, U, and vice-versa:

$U(t) = \Phi X(t)$,

and therefore obtain the corresponding uncoupled equilibrium equations:

$\ddot{X}(t) + \Phi^T C\Phi\dot{X}(t) + \Omega^2 X(t) = \Phi^T R(t)$, (2)

where $\dot{X}$ and $\ddot{X}$ are, respectively, the first and second order derivatives of the modal displacement vector and:

$\Phi^T K\Phi = \Omega^2$,

where I represents the identity matrix.

5. ESTIMATES

In this section we mention the solution adopted for some problems related to the lack of information about the objects and about the deformation involved. We will present the solutions found to estimate the initial displacement and velocity, as well as the nodes' implicit applied charges (successfully matched or not).

5.1 Initial Displacement and Velocity

The used integration method requires the initial displacement and velocity vectors. The solution found to estimate the first one is to consider it as a part of the expected modal displacement:

$$X_i^0 = c_X (X_{2,i} - X_{1,i}), \quad (3)$$

where X_i^0 represents the i^{th} component of the modal initial displacement, and c_X is a constraint defined by the user according to each application case.

Similarly, the initial modal velocity was estimated as a part of the initial modal displacement:

$$\dot{X}_i^0 = c_V X_i^0, \quad (4)$$

where c_V is also an user defined constraint.

As bigger values of c_X e c_V are used, larger are the obtained displacements and the target shape can be reached with fewer steps [9], [10]. Note that in the results to be presented, we have employed equal values of c_X and c_V for all nodes.

5.2 Implicit Applied Charges

The implicit applied charges on each matched node, i, are supposed to be proportional to the expected nodal displacement:

$$R_i = k(X_{2,i} - X_{j,i}), \quad (5)$$

where R_i is the applied charges' vector i^{th} component, $X_{2,i}$ is the i^{th} node's position in the target shape and $X_{j,i}$ in the j^{th} shape, and k is a global stiffness constraint (once again, considered equal for all components).

5.3. Unmatched Nodes

When all nodes aren't successfully matched, we can not use (5) and we have to estimate the implicit charges on the unmatched nodes by other means. So, we used the neighbourhood criterion according to which nodes must preserve their order during the deformation process: we apply on the unmatched nodes Horn's estimated global rigid transformation [6], [14]. Then we "link" each unmatched node's rigid transformed to its neighbour nodes that are within a predefined distance (figure 2).

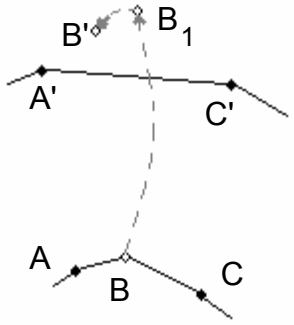

Figure 2: Used criterion to estimate the applied charges if *A* is matched with *A'*, *C* with *C'* and *B* is an unmatched node.

The initial displacement solution presented in (3) is also not defined for unmatched nodes. Once the implicit applied charges have been estimated, we recursively specify the initial displacement vector as part of the applied charges' vector. So:

$$\begin{cases} X_i^0 = \dfrac{c_X}{k} R_i & \text{if } k \neq 0 \\ X_i^0 = 0 & \text{if } k = 0 \end{cases}, \quad (6)$$

and, unless k is null, the initial modal displacement of the matched nodes equals (3). For each unmatched node of the first shape, the initial modal displacement is influenced, such as the implicit applied charges, by the nodes of the target shape that are near to the rigid transformed nodes.

It should be noticed that this solution is also based on the neighbourhood criterion.

6. EXPERIMENTAL RESULTS

The used approach was included in a software platform built to develop and test image processing and computer graphics algorithms (for a detailed presentation see [15]). That system integrates some public domain libraries as, for computer graphics algorithms, the *VTK – The Visualization Toolkit* [15], [16].

For the 2D shapes we considered contour objects to reduce the computational cost (although this methodology also works with inner objects' points, the results would be similar [6]).

For the first example consider contours 1 (composed by 32 nodes) and 2 (28 nodes), obtained from two real heart images [6]. We used polyethylene as virtual material, the global stiffness constraint $k = 2$, the time step $\Delta t = 1$, critical damping levels between 0.5% and 3%, and 75% of the modes in the LE resolution. Under these circumstances, if Sclaroff's isoparametric element is used then 16 nodes are matched (figure 3), and the final contour can be approached in 7 steps (figure 4); otherwise if grouped linear axial elements are used, 14 nodes are matched (figure 5) and the final contour is approached in 60 steps (figure 6).

Please note that the results presented with Sclaroff's element or with grouped axial elements probably are not the better ones. If we obtain a larger number of successful matches, the estimated shapes can be more realistic (figures 7 and 8).

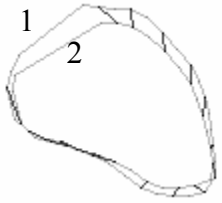

Figure 3: Matching between contours 1 and 2 when Sclaroff's element is used.

Figure 4: All intermediate shapes obtained with Sclaroff's element.

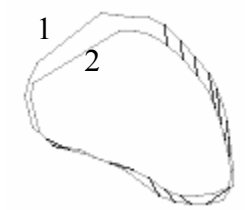

Figure 5: Matching between contours 1 and 2 when axial elements are used.

Figure 6: Intermediate shapes obtained in steps of 10 with axial elements.

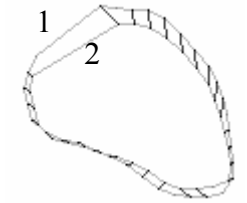

Figure 7: Matching between contours 1 and 2 when Sclaroff's element is used and 27 nodes are successfully macthed.

Figure 8: All intermediate shapes obtained with Sclaroff's element.

Now consider surfaces 3 (120 nodes) and 4 (107 nodes) obtained from two real heart images [6]. We used polyethylene as virtual material, the global stiffness constraint $k = 10$, and the same time step, critical damping and percentage of considered modes. When Sclaroff's isoparametric element is used to build the surfaces' models, 33 nodes are successfully matched as in figure 9. When grouped linear axial elements are used, only 8 nodes are matched (figure 12) and the intermediate shapes get closer to the target shape slowly (compare figures 10, 11, 13, 14). Once again, the obtained results can get better if a larger number of successful matches is obtained.

8. CONCLUSIONS AND FUTURE WORK

This paper proposes a physics-based approach to obtain the transitional shapes of image represented objects.

To build the given objects' models we used Sclaroff's isoparametric element or grouped linear axial elements. We verified that generally the models built by linear axial elements are more flexible and less dense than the ones built with the Sclaroff's element [6]. This can make it more difficult to do objects' deformation simulation, as the model is more elastic, witch can cause instability and so the obtained shapes may not converge to the target shape.

If all nodes of the given objects were successfully matched, then the implicit applied charges were considered as proportional to the distances between each node and its pair. But when not all the shapes' nodes were matched, we introduced a solution based on the neighbourhood criterion. So, for each unmatched node we applied the estimated rigid transformation between the given shapes and applied it to the unmatched nodes, then the obtained point is influenced by the matched nodes that are in a predefined distance.

In this paper the dynamic equilibrium equation has been solved using the Mode Superposition Method. This

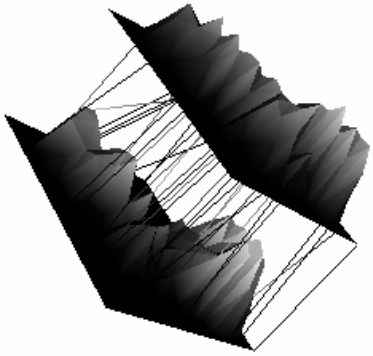

Figure 9: Modal Matching between surfaces 3 (left) and 4 (right) when Sclaroff's isoparametric element is used.

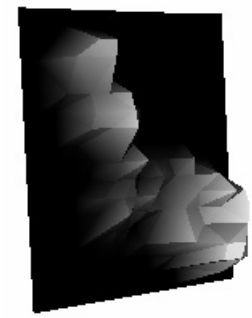

Figure 10: 5th Intermediate shape obtained with Sclaroff's element.

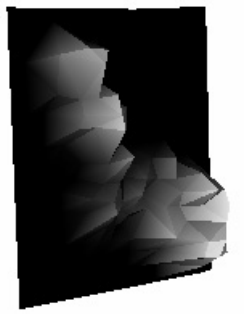

Figure 11: 10th Intermediate shape obtained with Sclaroff's element.

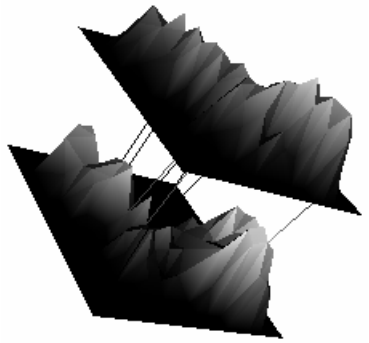

Figure 12: Modal Matching between surfaces 3 (left) and 4 (right) when grouped axial linear elements are used.

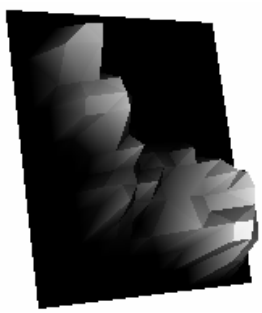

Figure 13: 5th Intermediate shape obtained with grouped axial linear elements.

Figure 14: 20th Intermediate shape obtained with grouped axial linear elements.

method allows that only a part of the model's modes are used, which reduces the computational effort (with accuracy decrease, but depending on the application's needs the obtained results may be satisfactory).

To apply the methodology proposed, it was necessary to estimate the implicit applied charges. The adopted solution can be improved through the search of alternative models to represent these charges (always attending to the possibility of unmatched nodes).

Another future task is the necessary validation of this methodology with real application examples. For example, in the domain of computer graphics this methodology may be used to simulate virtual reality, namely in the case of collision between deformable objects or to interpolate objects' data.

9. ACKNOWLEDGMENTS

The first author would like to thank the support of the PhD grant SFRH / BD / 12834 / 2003 of the FCT - Fundação de Ciência e Tecnologia in Portugal.

10. REFERENCES

[1] C. Nastar and N. Ayache, Fast Segmentation, Tracking, and Analysis of Deformable Objects. *4th. International Conference on Computer Vision*, Berlin, Germany, 1993, 275-279.

[2] C. Nastar, Modèles Phisiques Déformables et Modes Vibratoires pour l'Analyse du Mouvement non-rigide dans les Images Multidimensionnelles, *L'École Nationale des Ponts et Chaussées*, 1994.

[3] C. Nastar, N. Ayache, Frequency-Based Nonrigid Motion Analysis: Application to Four Dimensional Medical Images, *IEEE Transactions on Pattern Analysis and Machine Intelligence*, *18*, 1996, 1067-1079.

[4] S. Sclaroff, Modal Matching: A Method for Describing, Comparing, and Manipulating Digital Signals, *MIT*, 1995.

[5] S. Sclaroff, A. Pentland, Modal Matching for Correspondence and Recognition, *IEEE Transactions on Pattern Analysis and Machine Intelligence*, *17*, 1995, 545-561.

[6] J. Tavares, Análise de Movimento de Corpos Deformáveis usando Visão Computacional, *FEUP*, 2000.

[7] J. Tavares, J. Barbosa, and A. J. Padilha, Matching Image Objects in Dynamic Pedobarography. *RecPad'2000 - 11th Portuguese Conference on Pattern Recognition*, Porto, Portugal, 2000, 274-284.

[8] L. Meirovitch, *Elements of vibration analysis* (Mcgraw-Hill, 1986).

[9] R. Pinho, Determinação do Campo de Deslocamentos a partir de Imagens de Objectos Deformáveis, *Universidade do Porto*, 2002.

[10] R. Pinho, J. Tavares, Resolução da Equação Dinâmica de Equilíbrio entre Imagens de Objectos Deformáveis. *VII Congresso de Mecânica Aplicada e Computacional*, Évora, Portugal, 2003, 2109-2118.

[11] V. Foley, H. Feiner, *Computer graphics* (Addison-Wesley, 1991).

[12] K. Bathe, *Finite element procedures* (Prentice-Hall, 1996).

[13] R. Cook, D. Malkus, M. Plesha, *Concepts and applications of finite element analysis* (Wiley, 1989).

[14] B. Horn, Closed-Form Solution of Absolute Orientation using Unit Quaternions, *Journal of the Optical Society America A.*, *4*, 1987, 629-642.

[15] W. Schroeder, K. Martin, B. Lorensen, *The visualization toolkit*, (3rd. Edition, Kitware, 2002).

[16] W. Schroeder, K. Martin, *The VTK user's guide* (Kitware Inc., 2003).